Article

Not peer-reviewed version

Incorporation of Functionalized Amino Acid Ionic Liquid into Highly Porous MOF-177 to Improve Post-Combustion CO_2 Capture Capacity

Firuz A. Philip and Amr Henni *

Posted Date: 20 September 2023

doi: 10.20944/preprints202309.1349.v1

Keywords: CO2 Capture; Metal Organic Framework (MOF); Ionic Liquid; Amino Acid Ionic Liquid (AAILs); Task-Specific Ionic Liquid (TSIL); MOF-177

Article

Incorporation of Functionalized Amino Acid Ionic Liquid into Highly Porous MOF-177 to Improve Post-Combustion CO_2 Capture Capacity

Firuz A. Philip and Amr Henni *

Faculty of Engineering and Applied Science, University of Regina, Regina, SK, Canada; philip2f@uregina.ca
* Correspondence: amr.henni@uregina.ca

Abstract: This study presents the encapsulation of two amino acid-based ionic liquids (AAILs), 1-Ethyl-3-methylimidazolium glycine [Emim][Gly] and 1-Ethyl-3-methylimidazolium alanine [Emim][Ala], in a highly porous metal organic framework (MOF-177), to generate state-of-the-art composites for post-combustion CO_2 capture. The thermogravimetric analysis (TGA) demonstrated a successful encapsulation of the AAILs, consequently dramatically reducing the composites' surface area and pore volume. Both [Emim] [Gly]@MOF-177 and [Emim][Ala]@MOF-177 had close to 3 times the CO_2 uptake of MOF-177 at 20 wt.% loading, 0.2 bar, and 303 K. Additionally, 20-[Emim][Gly]@MOF-177 and 20-[Emim] [Ala]@MOF-177 enhanced their CO_2/N_2 selectivity from 5 (pristine MOF-177) to 13 and 11, respectively.

Keywords: CO2 capture; Metal Organic Framework (MOF); ionic liquid; amino acid ionic liquid (AAILs); task-specific ionic liquid (TSIL); MOF-177

1. Introduction

Metal-organic-frameworks, often known as MOFs, are a unique class of porous materials which are currently the subject of substantial research for a broad variety of applications [1,2], notably the storage and separation of gases, catalysis, and the delivery of drugs. MOFs are typically three-dimensional structures that have a high surface area and porosity. These structures are formed from metal nodes that are coupled with organic linkers. MOFs have lately gained an enormous amount of popularity for applications in CO_2 capture and storage because of their high porosity as well as their great potential for capture and, most significantly, due to their tunability [2–6]. Although some MOFs have displayed superb adsorbance of CO_2 at high pressure, at post-combustion conditions, in which the partial pressure of CO_2 is in general only about or lower than 0.15 bar, they showed very low CO_2 uptake. To enhance CO_2 capture capability, many strategies have been deployed including open metal sites [7], grafting amine functionalities covalently to the ligands [8–10], impregnation of amines [11–14], and the addition of ionic liquids (ILs) [15]. Physical impregnation of amines led to higher CO_2 uptake compared to covalent grafting of amines as more amine loading can be achieved by impregnation. Nonetheless, amine-impregnated sorbents are susceptible to amine loss, degradation, and high regeneration energy [16]. Ionic liquids (ILs) as an attractive alternative to amines have been proposed partly due to their low volatility and high thermal stability, however, it has been reported that in some cases, CO_2 uptake rather diminishes for ILs modified sorbents although improved selectivity was observed [17–19].

The first amine-functionalized ionic liquids (AILs) were developed by Bates et al. [20], demonstrating that the CO_2 sorption capacity of ILs can be substantially enhanced by functionalizing the sorbent with amine groups (-NH_2) while at the same time retaining IL properties. Since then, numerous AILs referred to as task-specific ionic liquids (TSILs) have been reported in the scientific literature. Among them, amino acid anion-functionalized ionic liquids (AAILs) have the clear advantages of an easy synthesis process, low cost, biodegradability, and using environmentally friendly raw materials as they are sourced from naturally occurring amino acids (AAs) [21–23]. As a result, AAILs are deemed promising candidates to functionalize porous MOF and lead to advanced

 doi:10.20944/preprints202309.1349.v1

sorbents with high CO_2 capture capacity. Several researchers have demonstrated that immobilization of AAILs into solid sorbents such as MCM-41, SBA-15 and PMMA led to an increase in carbon dioxide adsorption [24–27].

Recently, we showed that AAILs containing reactive Amino Acid (AA) anions such as Glycine [Gly] and Alanine [Ala] functioned as effective guest molecules in solid ZIF-8 support, significantly increasing CO_2 uptake and CO_2/N_2 selectivity [28]. Hence, we aim to expand our study to investigate new composites by impregnating these AAILs into MOF-177 as host sorbent, which is one of the highest porous MOFs reported to date with a pore volume of 1.69 cm^3/g and a BET-specific surface area of over 4000 m^2/g [29,30]. MOF-177 displays a 3D crystalline framework consisting of zinc metal clusters and 1, 3 , 5-benzene tribenzoate (BTB) organic linkers. Owing to its high porosity and volume, it displayed outstanding CO_2 uptake performance (60.8 wt.%) at high pressure (50 bar); however, CO_2 uptake at low pressure (0.15 bar) was very poor (0.6 wt.%) [16]. This led us to embark on this study and incorporate AAILs into highly porous MOF-177 forming AAILs@MOF-177 composites with improved active sorption sites, hopefully leading to a higher potential for CO_2 capture at post-combustion conditions. We are unaware of any prior work involving these composites. In this study, we investigated the composites and compared them to pure MOF-177 in terms of thermal stability, crystal structure, and textural qualities. The produced composites' potential in real-world CO_2 capture operations was investigated by investigating their CO_2 capture capacity, selectivity, and enthalpy of adsorption.

2. Results and Discussion

2.1. Characterizations of the AAILs-impregnated Sorbents

The thermogravimetric analysis of MOF-177 and AAILs@MOF-177 composites was performed to monitor the thermal stability of AAILs-supported MOF-177 composites from 25 to 800 °C in a nitrogen atmosphere. TGA thermograms of composites along with those of pure AAILs and pristine MOF-177 were presented in Figure 1a–d. The thermograms of pristine [Emim][Gly] and [Emim][Ala] indicate that both AAILs were thermally stable up to 200 °C, but beyond that temperature, a sharp weight loss was observed, indicating a very rapid decomposition. According to the derivative weight loss profile shown in Figure 1b,d, it was found that the onset decomposition temperatures (T_{onset}) were at about 215 °C and 225 °C, respectively. Whereas the pristine solid support MOF-177 was much more thermally stable than the pristine AAILs, with onset decomposition temperatures (T_{onset}) of about 421 °C in agreement with similar studies reported in the literature [30,31]. A little decrease in weight of around 2 to 4 wt.% was found in the composites at temperatures under 75 °C. This drop can be attributed to the potential evaporation of any residual methanol (BP 65 °C) that was employed during the synthesis of the composites. The thermogram of the composites revealed that the incorporated AAILs decomposed before the pristine solid support itself, as expected. However, note that there was no sharp decomposition of AAILs around the T_{onset} of AAILs, rather a gradual decomposition over the temperature range of 250 to 400 °C, and continued until MOF-177 itself started to decompose as displayed in Figure 1b,d. The gradual decomposition was more profound at higher loadings of AAILs such as 30-[Emim][Gly]@MOF-177 (Figure 1b) and 30-[Emim][Ala]@MOF-177 (Figure 1d). This progressive breakdown event could be attributed to the surface association that took place between MOF-177 and the incorporated AAILs.

Preprints (www.preprints.org) | NOT PEER-REVIEWED | Posted: 20 September 2023 doi:10.20944/preprints202309.1349.v1

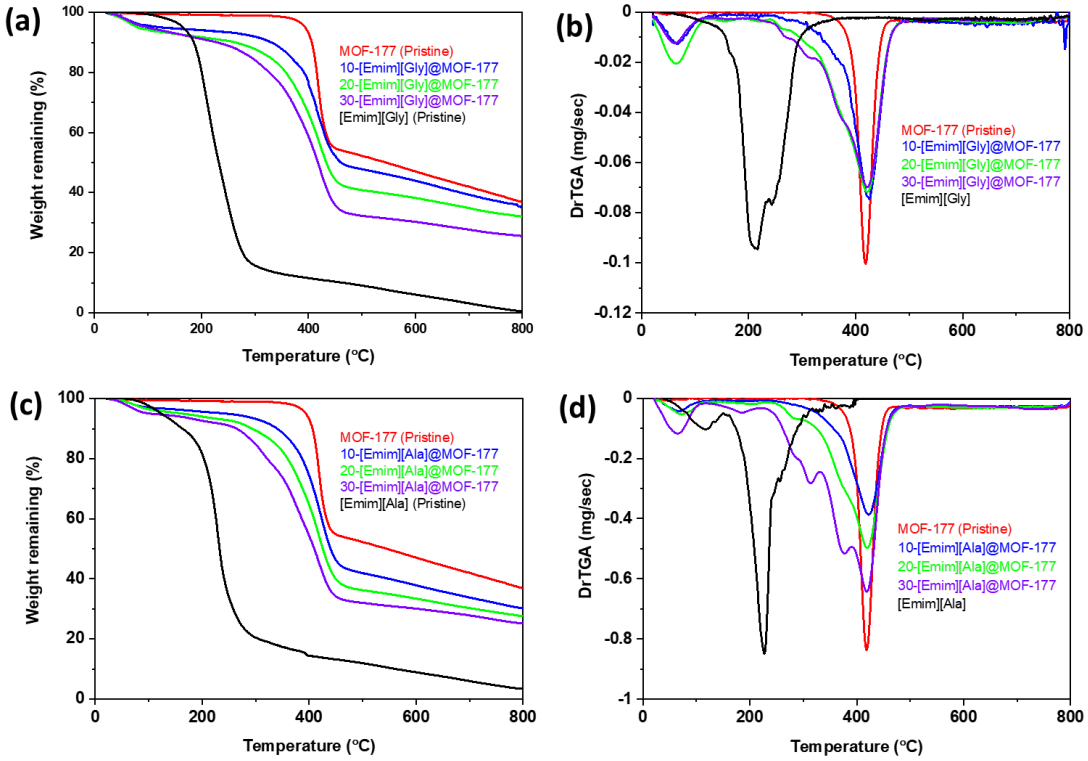

Figure 1. TGA thermograms and derivative of TGA profiles of the compounds [Emim][Gly]@MOF-177 (a-b) and [Emim][Ala]@MOF-177 (c-d).

In an attempt to determine the effect that encapsulated AAILs had on the solid support of MOF-177, the crystal structure of the composites was investigated utilizing X-ray diffraction (XRD), and the results of this investigation were illustrated in Figure 2. From the diffractogram of pristine MOF-177, the main characteristic peaks were at 5.5°, 6.2°, 9.6°, 10.4°, and 11.3°. A similar pattern was reported in the literature by Li and Yang [32], with a major peak at 5.2°, at 4.7° and 6.2 ° by Saha and Deng [31] and at 5.5° and 6.2° by Santos et al. [33]. As displayed in Figure 2a,b, the XRD of the composites revealed that the impregnation of AAILs into the MOF-177 support had a significant impact on peak intensity and position. For a small loading of 10 wt.% for both [Emim][Gly] and [Emim][Ala], the prominent characteristic peaks were at 5.5°, 6.2°, 9.6°for pristine MOF-177 and have therefore significantly declined but peaks at 11.1°and 11.7° retained their intensity with a minor shift from the original positions. It was evident that the intensity of major peaks diminished with the increment of AAILs loading and eventually almost disappeared at a loading of 30 wt.%, as displayed for both 30-[Emim] [Gly]@MOF-177 and 30-[Emim][Ala]@MOF-177, suggesting some morphological changes. The existence of the guest molecules and their interaction with the host solid support account for the observed behavior. A similar complete disappearance of all the major characteristic peaks of MOF-177 due to the presence of chloroform was reported by Saha and Deng [31] and according to the authors, the occupying guest molecules in the pore of MOF-177 caused a shift in the atomic orientation in the crystal planes. The TGA thermograms discussed in the preceding section confirmed that there was a significant interaction between AAILs and MOF-177 support. Overall, the XRD data indicated the occurrence of morphological changes in AAILs@MOF-177 composites, especially for a loading higher than 20 wt. %.

Preprints (www.preprints.org) | NOT PEER-REVIEWED | Posted: 20 September 2023 doi:10.20944/preprints202309.1349.v1

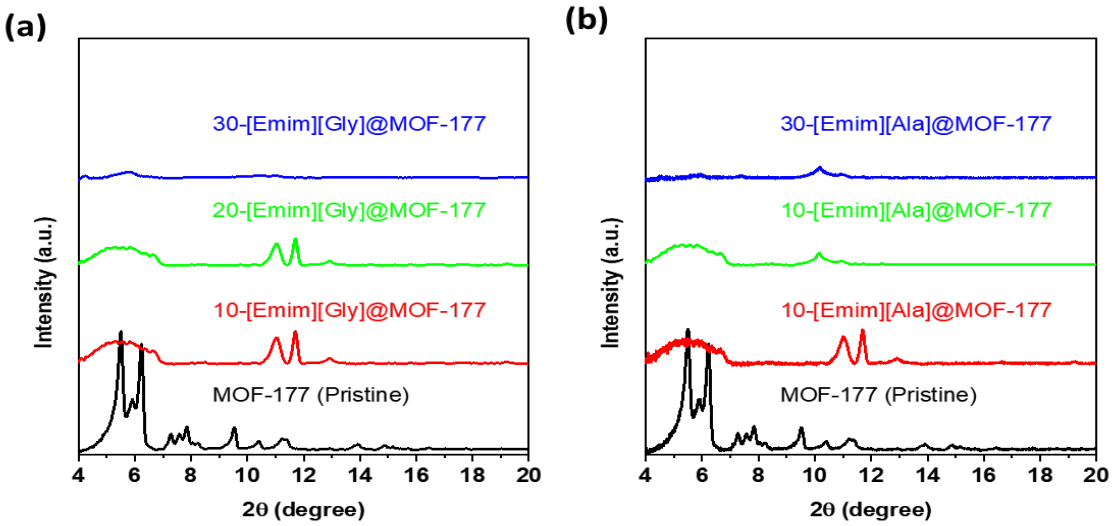

Figure 2. XRD profile of pristine MOF-177 and composites: (a) Emim][Gly]@MOF-177; (b) [Emim][Ala]@ MOF-177.

To further assess the impact of the incorporation of AAILs on the textural properties of MOF-177 support, N_2 adsorption-desorption isotherms were obtained under a liquid nitrogen environment (77 K) using the ASAP 2460 (Micromeritics) for the unmodified MOF-177 and AAILs@MOF-177 composites, and the isotherms were presented in Figure 3. The samples' specific surface areas were determined at relative pressures (P/P0) between 0.04 and 0.1 bar using the Brunauer-Emmett-Teller (BET) model. The Langmuir correlations and calculated results are presented in Table 1. The pristine MOF-177 showed significantly higher N_2 uptake, and the isotherm profile corresponded to a reversible Type I isotherm (IUPAC classification) which was indicative of a microporous material lacking hysteresis during desorption. BET and Langmuir surface areas of pristine MOF-177 were 4172 $m^2 \cdot g^{-1}$ and 4962 $m^2 \cdot g^{-1}$, respectively, which were close to the reported values by Yaghi's group [29]. Both BET and Langmuir surface areas of MOF-177 reported in the literature varied significantly from 3100 – 4962 $m^2 \cdot g^{-1}$ and 4300 – 5994 $m^2 \cdot g^{-1}$, respectively [29,31,32,34]. It is observed from Figure 3 that N_2 adsorption in all composites was significantly lower than in the pristine MOF-177 which was evidence of a substantial drop in surface area as well as pore volume (Table 1). For instance, upon impregnation of 10 wt.% [Emim][Gly] and [Emim][Ala], BET surface area as reduced to only 187 $m^2 \cdot g^{-1}$ and 152 $m^2 \cdot g^{-1}$, respectively. The surface area and pore volume of the composites were further reduced with the addition of AAILs. The BET surface areas and pore volumes obtained for a 30 wt.% loading of [Emim][Gly] have been estimated to be 27 $m^2 \cdot g^{-1}$ and 0.02 $cm^3 \cdot g^{-1}$, respectively. These results indicate that the pores were almost filled. It should be acknowledged that the [Emim][Gly]@MOF-177 composites exhibited somewhat greater surface area and pore volume compared to the [Emim][Ala]@MOF-177 composites. The reduction of surface area and pore volume confirmed that the AAILs were encapsulated into the pores of MOF-177. However, the severe decline in both surface area and pore volume especially for higher loading of AAILs can be attributed to possible structural and morphological changes due to the collapse of some of the MOF-177 structure which was also apparent in the XRD results discussed earlier.

Preprints (www.preprints.org) | NOT PEER-REVIEWED | Posted: 20 September 2023 doi:10.20944/preprints202309.1349.v1

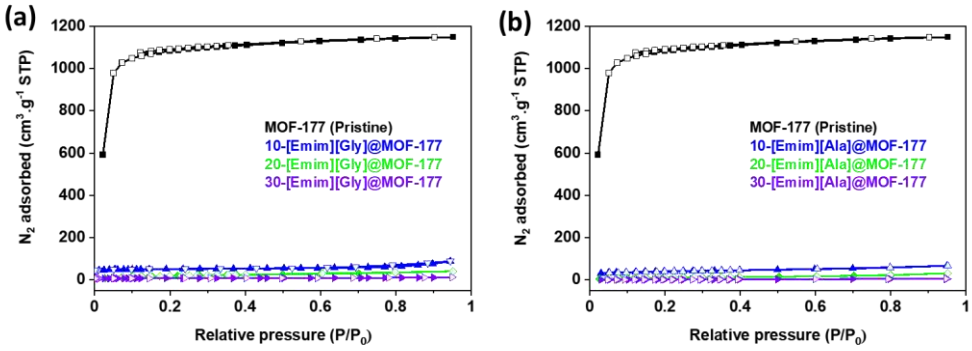

Figure 3. N_2 adsorption-desorption isotherms at 77 K for unmodified MOF-177 and composites: (a) [Emim][Gly]@MOF-177 (b) [Emim][Ala]@MOF-177. Filled and unfilled symbols represented the adsorption and desorption isotherms, respectively.

Table 1. Textural properties of pristine MOF-177 and AAILs@ MOF-177 composites computed from the N_2 adsorption-desorption isotherms at 77.

Samples	S_{BET} ($m^2 \cdot g^{-1}$)	$S_{Langmuir}$ ($m^2 \cdot g^{-1}$)	Pore Volume ($cm^3 \cdot g^{-1}$)
MOF-177	4172	4962	1.78
10-[Emim][Gly]@MOF-177	187	250	0.13
20-[Emim][Gly]@MOF-177	74	147	0.06
30-[Emim][Gly]@MOF-177	27	41	0.02
10-[Emim][Ala]@MOF-177	152	226	0.10
20-[Emim][Ala]@MOF-177	39	89	0.05
30-[Emim][Ala]@MOF-177	9.3	29	0.01

2.2. CO_2 Adsorption Isotherms

MOF-177 is one of the highest porous MOFs reported to date in the open literature, and as a result, it has higher adsorption capacity at high pressure. However, its adsorption capacity at post-combustion conditions (up to 0.15 bar) was very low [16]. The current investigation involved the synthesis of composites including [Emim][Gly]@MOF-177 and [Emim][Ala]@MOF-177. These composites were prepared by introducing two amino acid anion-functionalized ionic liquids (AAILs), commonly referred to as task-specific ionic liquids (TSILs), into the MOF-177 using the wet impregnation method. These composites' equilibrium CO_2 uptakes were determined at 30, 40, and 50 °C. Each isotherm covered pressures between 0.1 and 10 bar. Figure 4 shows the equilibrium CO_2 uptake in pure MOF-177 and [Emim][Gly]@MOF-177 for pressure spanning from 0.1 to 10.0 bar (Figure 4a,c,e) and a narrower pressure range (Figure 4b,d,f) spanning from 0.1 to 1.0 bar. The addition of [Emim][Gly] to MOF-177 increased its ability to adsorb CO_2 at low pressures between 0.1 and 1.0 bar. When compared to pristine MOF-177 and all other [Emim][Gly]@MOF-177 composites at all temperatures, CO_2 adsorption capacity increased dramatically with the incremental addition of AAILs loading and peaked at a loading of 20 wt%. At 0.2 bar and 303 K, the CO_2 adsorption for 20-[Emim][Gly]@MOF-177 was 0.45 $mmol \cdot g^{-1}$ solid, which was three times that of the pristine MOF-177 under the same circumstances. However, increasing the TSIL amount to 30 wt.% failed to result in a noticeable rise in CO_2 uptake; rather, a decrease in CO_2 uptake to 0.26 $mmol \cdot g^{-1}$-solid was observed when compared to 20 wt.% loading, even though it was a bit higher when compared to pure MOF-177 at the same conditions. It is noteworthy that the carbon dioxide absorption capacity of all composites consisting of [Emim][Gly]@MOF-177 exhibited a decrease in performance at the given temperature, in comparison to the pure MOF-177, when the pressure exceeded 2 bar. CO_2 uptake by all composites decreased when the temperature was elevated from 30 °C to 40 °C and 50 °C while maintaining the same pressure.

Preprints (www.preprints.org) | NOT PEER-REVIEWED | Posted: 20 September 2023 doi:10.20944/preprints202309.1349.v1

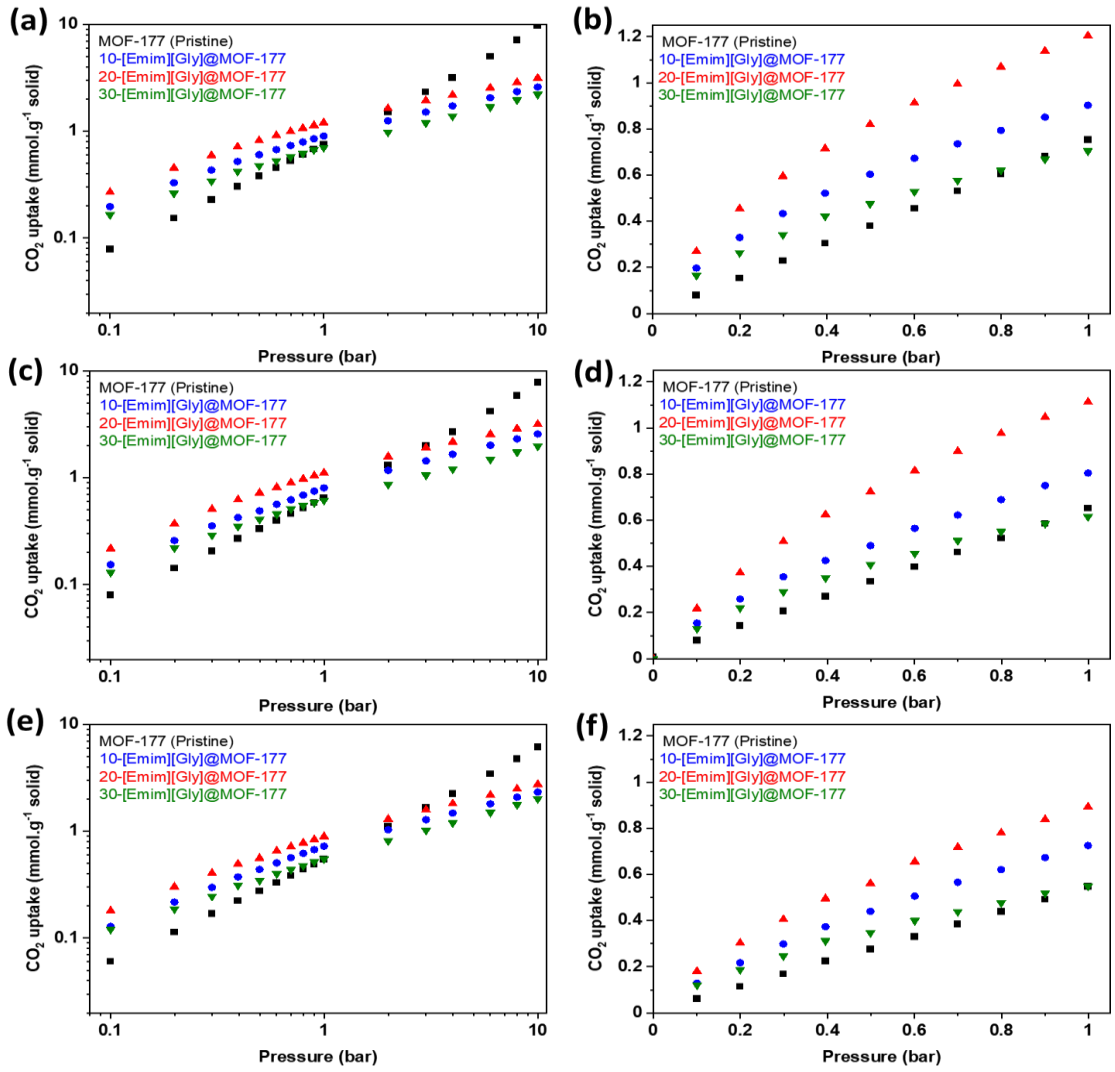

Figure 4. The CO_2 equilibrium adsorption capacity of [Emim][Gly]@MOF-177 composites at two pressure ranges (0-10 bar and 0-1 bar) at three temperatures: (a & b) at 303 K, (c & d) at 313 K, and (e & f) at 323K.

Figure 5 shows the equilibrium CO_2 uptake in the pure MOF-177 and [Emim][Ala]@MOF-177 for pressure spanning from 0.1 to 10.0 bar (Figure 5a,c,e) and a narrower pressure range (Figure 5b,d,f) spanning from 0.1 to 1.0 bar. It demonstrated that the incorporation of [Emim][Ala] had a favourable CO_2 adsorption capability for pressure below 2 bar and followed exactly a similar trend of [Emim][Gly]@MOF-177 composites. 20-[Emim][Ala]@MOF-177 outperformed all other [Emim][Ala]@MOF-177 composites and pure MOF-177 in CO_2 capture capacity. This composite reached up to 0.42 mmol·g^{-1} solid at 0.2 bar and 303 K, which was nearly three times higher compared to the unaltered MOF-177 under the same conditions. When the loading of [Emim][Ala] was raised to 30 wt.%, CO_2 capture capacity dwindled, and the resulting values were in the middle of the range for capture capacity at 10 and 20 wt.% loading. It was worth noting that under identical temperature and pressure, the CO_2 adsorption capacity of [Emim][Ala]@MOF-177 composites was slightly lower than the [Emim][Gly]@MOF-177 composites with the same AAIL loading.

Preprints (www.preprints.org) | NOT PEER-REVIEWED | Posted: 20 September 2023 doi:10.20944/preprints202309.1349.v1

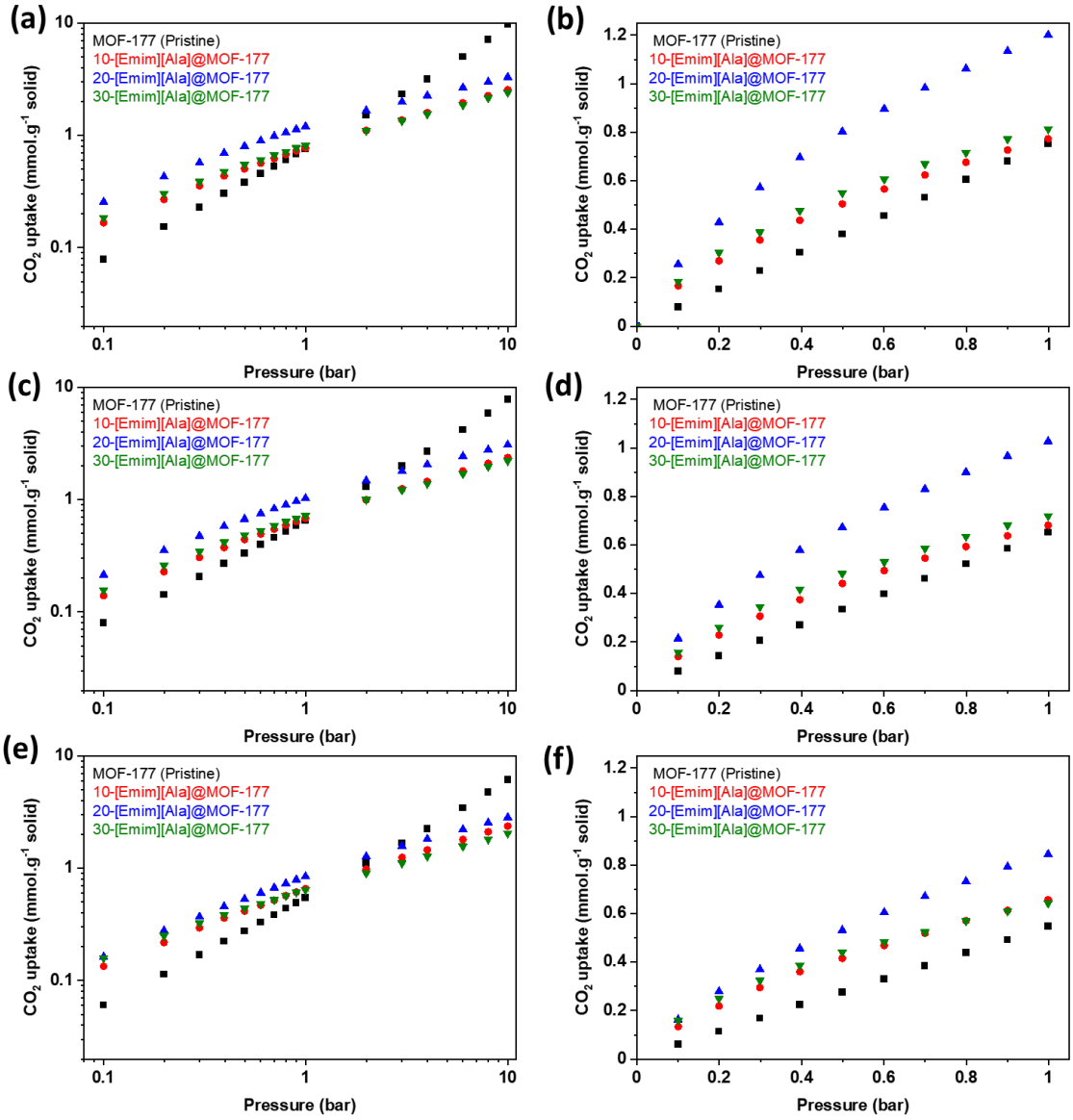

Figure 5. The CO_2 equilibrium adsorption capacity of [Emim][Ala]@MOF-177 at two pressure ranges (0-10 bar and 0-1 bar) and three temperatures: (a & b) at 303 K, (c & d) at 313 K, and (e & f) at 323K.

The introduction of [Emim][Gly] and [Emim][Ala] AAILs to the MOF-177 sorbent led to a notable enhancement in CO_2 adsorption under post-combustion circumstances ($P_{CO2} \approx 0.15$ bar) due to the strong attraction between CO_2 and the amino group present in AAILs. Previous research indicated that the amino group of AAILs reacted with CO_2 via a process analogous to that of amines dissolved in water [20,35,36]. Wang et al. [37] suggested that as the cation and anion of [Emim][Gly] were small in size, they could therefore come nearby an amino group and reacted to form a carbamate with a stoichiometry of 1:2. Hence, it was reasonable to assume that the amino group present in these composites reacted with CO_2 to form carbamate, resulting in a higher CO_2 capture capacity than pure MOF-177 below 1 bar.

It is noteworthy to mention that, when the pressure is below 1 bar, chemical adsorption becomes the prevailing factor. This is attributed to the strong affinity between CO_2, and AAILs. Consequently, the CO_2 adsorption capacity is enhanced. However, it is important to note that the occupation of MOF-177 pores by AAILs molecules leads to a significant reduction in the available surface area of the composites. Nevertheless, as the pressure escalated, the composites' advantage waned, resulting

Preprints (www.preprints.org) | NOT PEER-REVIEWED | Posted: 20 September 2023 doi:10.20944/preprints202309.1349.v1

in a CO_2 uptake that was lower than that of the pristine MOF-177 at pressures exceeding 2 bar. This decline can be due to the significant reduction in pore volume as well as the surface area of the composites. In the context of moderate to high pressure, the adsorption capacity of the sorbent is primarily influenced by physical adsorption sites, in addition to the active chemical adsorption sites [38].

Our experimental results revealed that there was an upper limit to the loading of AAILs which was found to be 20 wt.% and beyond the limit, CO_2 uptake decreased. This phenomenon of reduction in CO_2 capacity which is ascribed to the reduction of accessible active sites of the sorbent due to the blockage or collapse of the MOF-177 support at high AAIL concentrations, which was also evident in the XRD, BET surface area, and pore volume results of 30% AAILs@MOF-177 as discussed earlier. An analogous finding in trend was reported by Wang et al. [37] for the impregnation of [Emim][Gly] into the nanoporous structure of polymethylmethacrylate (PMMA) by varying the loading from 0 to 100 wt.% and the optimum loading was found to be 50 wt.%. In another study, Uehara et al. [26] reported that the optimum loading of [Emim][Lys] was 60 wt.% for the mesoporous silica support of SBA-15.

The stability of the composites in the CO_2 capture operation was investigated by performing multiple cycles of adsorption at 313 K and desorption cycles at 373 K at atmospheric pressure in the presence of N_2 for 20 wt.%-[Emim][Gly]@MOF-177 using the IGA microbalance. The obtained results are displayed in Figure 6. They showed that the composite sorbent can almost maintain its original adsorption capacity during multicycle operations. In addition, the CO_2 uptake process for AAILs@MOF-177 was completely reversible suggesting that the composites can be readily regenerated in the presence of flowing N_2 at 100 °C.

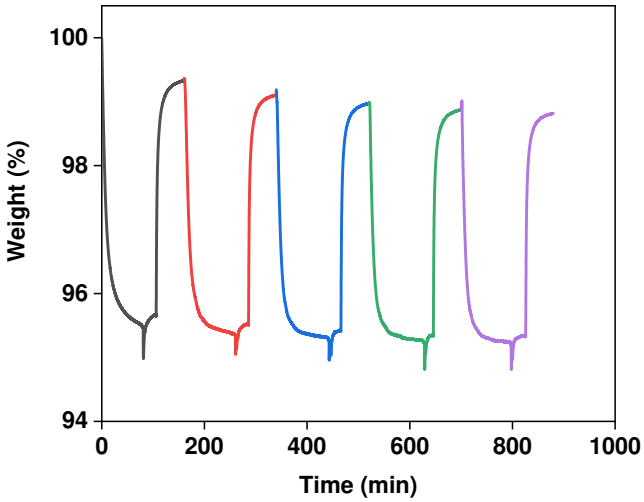

Figure 6. Adsorption and desorption performance during multiple cycles for 20 wt.% [Emim][Gly]@MOF-177 composite. Adsorption was conducted at 313 K and desorption at 373 K in the presence of N_2 flow.

2.3. Selectivity for CO_2/N_2

To be deemed effective in the post-combustion capture of carbon dioxide (CO_2), a solid sorbent must have a notable level of selectivity towards CO_2 when compared to nitrogen (N_2). Consequently, the determination of N_2 adsorption isotherms at a temperature of 40 °C was undertaken to quantify the CO_2/N_2 selectivity. Each isotherm encompassed a range of pressures ranging from 0.1 to 10 bar. In our current study, we employ a particular methodology to determine the optimal selectivity. our strategy entails calculating the selectivity by comparing the molar uptakes of individual components at a given pressure, as indicated in Equation (1) [2].

$$S = \frac{q_{CO2}}{q_{N2}} \quad (1)$$

Preprints (www.preprints.org) | NOT PEER-REVIEWED | Posted: 20 September 2023 doi:10.20944/preprints202309.1349.v1

where S denoted the selectivity and q_{CO2} and q_{N2} represented the molar uptakes of CO_2 and N_2, respectively. Figure 7 presents the results of the calculations made on the CO_2/N_2 selectivity for both [Emim][Gly]@MOF-177 and [Emim][Ala]@MOF-177 composites. Throughout the whole pressure spectrum, the CO_2/N_2 selectivity of pure MOF-177 fluctuated somewhere between three and five. It was discovered that the impregnation of [Emim][Gly] and [Emim][Ala] into MOF-177 boosted the selectivity for all loadings compared to the virgin MOF-177 up to a pressure of 2 bar. Regarding the composites involving [Emim][Gly]@MOF-177, it was observed that the compound 20-[Emim][Gly]@MOF-177 demonstrated the highest selectivity, reaching around 13 at a pressure of 0.2 bar and a temperature of 313 K. Nevertheless, the observed value exhibited a gradual decline as the pressure was raised, as depicted in Figure 7a. It is important to note that the increase in loading to 30-[Emim][Gly] did not increase selectivity; rather, it resulted in a selectivity that was worse than that at 10 wt.%, except at 0.1 bar. Similar behaviour was seen for [Emim][Ala]@MOF-177 composites, with the maximum selectivity of around 15 (0.1 bar) and 11 (0.2 bar) displayed by 20-[Emim][Ala]@MOF-177. It was discovered, however, that the selectivity of a 30-[Emim][Ala]@MOF-177 composite is nearly identical to that of a 20-[Emim][Ala]@MOF-177 composite.

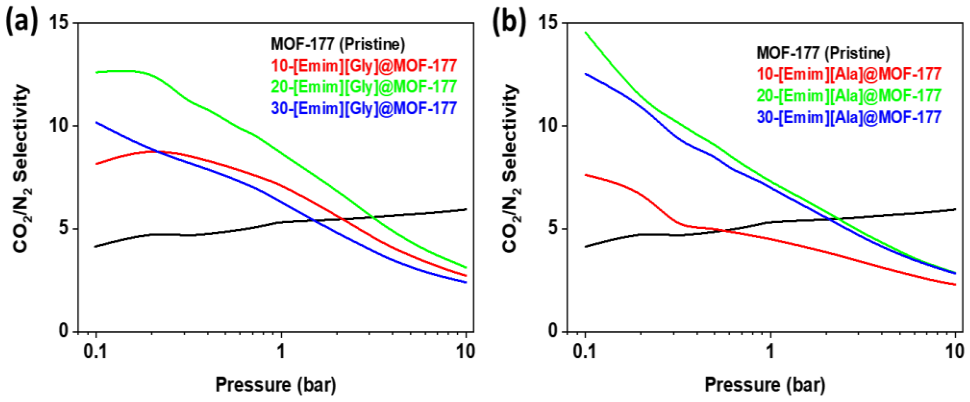

Figure 7. CO_2/N_2 selectivity of [Emim][Gly]@MOF-177 (a) and [Emim][Ala]@MOF-177 (b) composites at 313 K.

The encapsulated amino acid-base ionic liquids contributed to the enhancement of CO_2/N_2 selectivity. This improvement was observed at pressures below 2 bars. As previously discussed, it has been proposed that the existence of amino acids leads to the formation of active chemical sorption sites for CO_2, facilitating the creation of an N-C bond. This interaction is similar to the way CO_2 interacts with an aqueous amine solution [39]. This resulted in additional CO_2 capture, although the surface area and pore volume were reduced due to the addition of the ionic liquid. On the other hand, N_2 did not have an affinity for the amino group as the adsorption was physical and depended on the available surface area. Hence, CO_2 uptake was dominant at low pressure compared to N_2, resulting in higher CO_2/N_2 selectivity. However, as the pressure increased, the physical adsorption sites also became the determining factors of the adsorption capacity besides the active chemical adsorption sites in the sorbent. Consequently, the CO_2/N_2 selectivity of composites decreased as pressure increased and became lower than the unmodified MOF-177 for pressures above 2 bar.

2.4. Equilibrium Isotherm Modeling

To accurately represent the outcomes of the experimental investigations pertaining to the design of adsorption and desorption processes, it was imperative to construct a model of the equilibrium isotherm. The presence of encapsulated AAILs within the pore structure of MOF-177 resulted in the composite material under investigation exhibiting binding sites of varying strengths. After conducting a comparative analysis with various existing models, it was determined that the Dual-Site-Langmuir (DSL) model [18,40] had a high level of suitability. The model incorporates the

Preprints (www.preprints.org) | NOT PEER-REVIEWED | Posted: 20 September 2023 doi:10.20944/preprints202309.1349.v1

Langmuir adsorption mechanism, which involves two distinct adsorption sites. The overall adsorption is determined by the cumulative effect of adsorption occurring at each individual site, as represented by Equation (2) [39].

$$N_e = \frac{N_A b_A P}{1 + b_A P} + \frac{N_B b_B P}{1 + b_B P} \quad (2)$$

In the DSL model, the equilibrium intake of CO_2 (N_e) is denoted in millimoles per gram of solid, while the equilibrium pressure (P) is given in bar. The parameters N_A, N_B, b_A, and b_B were utilized in this model. The regressed parameters for the composites are presented in Tables 2 and 3. These tables include the parameters obtained from the regression analysis for different loadings of ionic liquids (ILs) at various temperatures. Figures 8 and 9 provide visual representations of the fitting curves generated by the DSL model. Due to the R^2 values exhibiting a high degree of proximity to unity, it can be inferred that the model effectively achieved a remarkable level of conformity with the experimental data. Consequently, the data obtained from the model will be utilized to compute the heat of adsorption in the subsequent section.

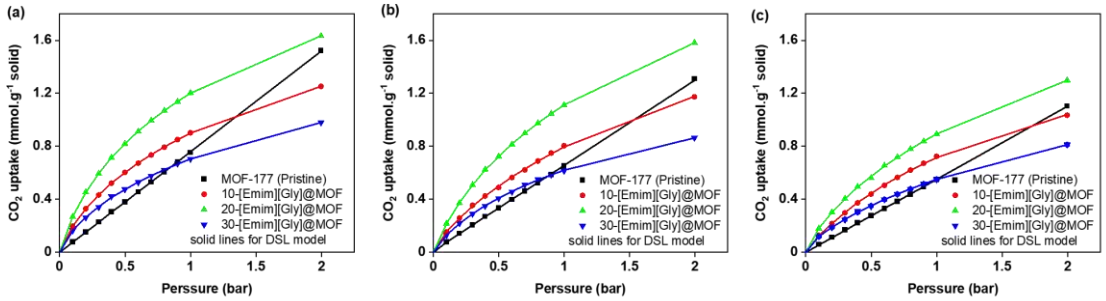

Figure 8. Fitting of DSL model for MOF-177 and [Emim][Gly]@ MOF-177 composites at different loading of AAILs at 30 °C (a), 40 °C (b) and 50 °C (c) for pressure spanning from 0.1 to 2.0 bar.

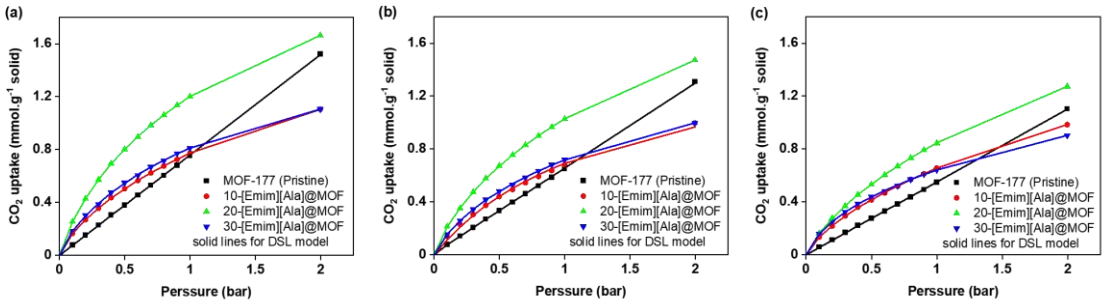

Figure 9. The Fitting of DSL model for MOF-177 and [Emim][Ala]@ MOF-177 composites with different loading of AAILs at 30 °C (a), 40 °C (b), and 30 °C (c) for pressure spanning from 0.1 to 2.0 bar.

Table 2. Computed parameters of DSL model for [Emim][Gly]@MOF-177 composites with different loading of AAILs for pressure spanning from 0.1 to 2.0 bar.

Model Parameters	10-[Emim][Gly]@ MOF-177			20-[Emim][Gly]@MOF-177			30-[Emim][Gly]@MOF-177		
	30 °C	40 °C	50 °C	30 °C	40 °C	50 °C	30 °C	40 °C	50 °C
N_A	2.019	2.350	1.921	0.436	0.292	0.165	1.590	0.097	0.087
b_A	0.514	0.426	0.562	5.117	4.698	9.030	0.508	10.678	18.396
N_B	0.247	0.098	0.024	2.371	2.694	2.444	0.190	1.405	1.628
b_B	6.692	15.04	10000	0.545	0.479	0.439	8.468	0.609	0.404
R^2	1.000	1.000	1.000	1.000	1.000	1.000	1.000	1.000	1.000

Preprints (www.preprints.org) | NOT PEER-REVIEWED | Posted: 20 September 2023 doi:10.20944/preprints202309.1349.v1

Table 3. Computed parameters of DSL model for [Emim][Ala]@MOF-177 composites with different loading of AAILs for pressure spanning from 0.1 to 2.0 bar.

Model Parameters	10-[Emim][Ala]@ MOF-177			20-[Emim][Ala]@MOF-177			30-[Emim][Ala]@MOF-177		
	30 °C	40 °C	50 °C	30 °C	40 °C	50 °C	30 °C	40 °C	50 °C
N_A	1.960	0.000	0.151	0.306	0.230	2.791	1.698	1.602	0.246
b_A	0.501	0.000	7.765	6.003	7.147	0.326	0.697	0.539	7.046
N_B	0.129	1.600	2.182	2.607	2.618	0.185	0.122	0.180	1.599
b_B	12.735	0.763	0.315	0.564	0.462	6.700	15.549	6.987	0.365
R^2	1.000	0.999	1.000	1.000	1.000	1.000	1.000	1.000	1.000

2.5. Isosteric heat of adsorption (Q_{st})

The determination of the adsorption enthalpy of carbon dioxide (Q_{st}), referred to as the isosteric heat of adsorption, plays a pivotal role in the adsorption process. It displayed the gas molecules' affinity for the adsorbents and the degree of their interaction with them. The energy requirements for the adsorption-desorption process were therefore quantified. CO_2 isotherms at 303, 313, and 323 K were used to calculate the adsorption enthalpy (Q_{st}). At first, the DSL model was employed to establish a suitable match for the isotherms, as elucidated in the preceding section. Subsequently, the Clausius-Clapeyron equation (3) was utilized [39].

$$(\ln P)_N = -\left(Q_{st}/R\right)\left(1/T\right) + C \quad (3)$$

In the given context, the symbol P denotes the pressure in units of bar, N represents the extent of CO_2 adsorption, T signifies the temperature measured in Kelvin (K), and R denotes the universal gas constant. The equation was utilized to produce graphs depicting the natural logarithm of the partial pressure (ln P) as a function of the reciprocal of temperature (1/T) while maintaining a constant rate of carbon dioxide consumption. The value of Q_{st} was then determined by calculating the slope of these plots. The findings are depicted in Figure 10, illustrating the outcomes for both pure MOF-177 and AAILs@MOF-177.

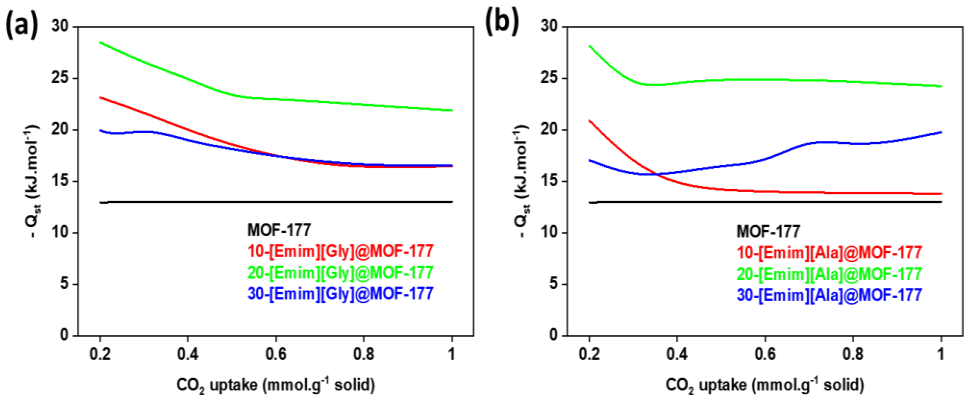

Figure 10. The enthalpy of CO_2 adsorption (Qst), of the composites (a) [Emim][Gly]@MOF-177 and (b) [Emim][Ala]@MOF-177.

Q_{st} values for the pure MOF-177 remained relatively stable at 13 kJ·mol^{-1}, in contrast, a significant rise in Q_{st} was observed for the composites, particularly at low levels of CO_2 uptake. When compared to other [Emim][Gly] composites, 20-[Emim][Gly]@MOF-177 showed the highest values for Qst, reaching a maximum of -28 kJ·mol^{-1} at 0.2 mmol·g^{-1} CO_2 uptake. This value was double that of pure MOF-177 under identical conditions [Figure 10a]. Similarly, it was observed that the composite material 20-[Emim][Ala]@MOF-177 displayed the most significant Q_{st} values compared to other

composites of [Emim][Ala]@MOF-177 [Figure 10b]. The significant increase in Q_{st} can be ascribed to the strong intermolecular forces between carbon dioxide (CO_2) and the ionic liquids that have been incorporated within the pores of MOF-177. There exists a hypothesis suggesting that the anions of AAILs, containing the -NH_2 group, undergo a reaction to form an N-C bond. This reaction is believed to contribute to the higher heat release observed after the adsorption of CO_2 [39]. The decrease in the quantity of available adsorption sites can be attributed to the observed decline in the Q_{st} value across all composites, which coincided with an increase in CO_2 uptake. A similar observation was reported for a composite of MIL-100 (Fe) modified with DETA [11]. As expected, Q_{st} for both 30%-[Emim][Gly]@MOF-177 and 30%-[Emim][Ala]@MOF-177 were in between 10 and 20 wt.% loading, which confirmed the CO_2 adsorption isotherm and selectivity pattern observed and discussed in the previous section.

3. Materials and Methods

3.1. Materials

Sigma Aldrich supplied the methanol (CAS 67-56-1), [Emim][Gly] (CAS 766537-74-0), [Emim][Ala] (CAS 766537-81-9) and the MOF-177 (Basolite Z377, CAS: 676593-65-0). Before beginning sample preparation, MOF-177 was allowed to dry overnight at 110 ^{o}C. All other compounds were used just as supplied. To reduce the amount of time that the samples were exposed to moisture, the ionic liquid, MOF-177, and the produced composites were stored in a glovebox (Clean Tech LLC) filled with argon gas. Praxair Inc. Canada was the supplier of the CO_2 and N_2 that had a high purity level (99.99 vol.%).

3.2. Preparation of AAIL@MOF-177 composite

Using the wet impregnation approach and methanol as a solvent, amino acid ionic liquids [Emim][Gly] and [Emim][Ala] were effectively embedded within the porous MOF-177 support. In summary, the desired amount of AAILs was added to 4 ml of methanol in a small glass vial, and the mixture was made homogenized by shaking it for 30 minutes. The AAIL-methanol solution was carefully added in a dropwise manner to the pre-weighed dehydrated MOF-177, which was contained in a separate glass vial. The resulting combination was then agitated for 1 hour. Following 24 hours of solvent evaporation under ambient conditions, any residual solvent was then removed by subjecting the composite to a drying process at a temperature of 80 °C for 2 hours. The created composite samples were stored in an argon-filled glovebox to prevent exposure to moisture and were labelled as X-AAILs@MOF-177, in which X represents the weight % of AAILs used; for instance, 10 wt.% [Emim][Gly] will be referred to as 10-[Emim][Gly]@MOF-177.

3.3. Characterization

The thermogravimetric analysis (TGA) of [Emim][Gly], [Emim][Ala], pristine MOF-177, and all synthesized AAILs@MOF-177 composites was conducted with a Shimadzu Thermal Gravimetric Analysis device (TGA-50). The analysis was performed using a nitrogen flow rate of 50 mL/min with the temperature gradually increasing to 800 ^{o}C at a rate of 10 ^{o}C/min. In each of the analyses, a sample size of roughly 10 to 12 mg was utilized. To analyze the crystal structure of pure MOF-177 support as well as AAILs@MOF-177 composites, a tabletop X-ray diffraction (XRD) device (Rigaku Miniflex-II) was employed. The Cu Ka radiation used in this experiment had a wavelength of 1.5418 Å. The examination was carried out at a scanning step of 1.2 ^{o}C/min between 2θ values of 2 and 20 degrees, a temperature of 77 K and using an instrument manufactured by Micromeritics ASAP. The N_2 adsorption and desorption isotherms of MOF-177 and as-synthesized composites were determined. Based on the data from the N_2 isotherm, the textural features of each sample, such as the surface area (BET and Langmuir), as well as the pore volume, were computed.

 doi:10.20944/preprints202309.1349.v1

3.4. Adsorption Isotherms

An intelligent gravimetric analyzer (IGA-003), manufactured by Hidden Isochema Ltd., was utilized to acquire CO_2 adsorption data at 303, 313, and 323 K, as well as N_2 adsorption data at 313 K, throughout a wide span of pressures ranging from 0.1 bar to 10 bar. The IGA consisted of a computer-controlled microbalance that measured the weight in real-time with a precision of 1 μg. Between 50 and 70 mg of material were deposited into a sample bucket for each isotherm. After heating the sample chamber to 80 °C using a water bath and vacuuming to 10 mbar with a diaphragm and turbo-pump (Pfeiffer), the sample weight stayed constant for 1 hour, indicating that all the solvent, moisture, and contaminants were removed. Following the completion of the outgassing process, the temperature of the water bath was adjusted to the predetermined isotherm temperature, and subsequently, the sample was permitted to attain the designated temperature. Once the sample was ready, pressure levels were pre-set to a value ranging from 0.1 to 10 bar in the IGASwin software, and the isotherm measurements were initiated. A mass flow controller (MFC) was used to regulate the quantity of CO_2 or N_2 injected into the chamber to maintain the desired pressure. The IGASwin program kept track of the real-time measurements of mass, temperature, and pressure. After allowing each pressure level to establish equilibrium for at least two hours and recording the results, more CO_2 or N_2 was injected via the MFC at the following pressure level. At a given temperature, this procedure was repeated for each of the predetermined pressures. After the experiment was complete, the buoyancy effect was accounted for in the real-time adsorption data.

3.5. Cyclic adsorption-desorption test

At 40 °C and 1 bar, the IGA was used to perform cyclic CO_2 adsorption and desorption studies. As explained earlier, before the adsorption sample was degassed and the temperature adjusted to 40 °C. After 30 minutes of temperature stabilization, the injection of carbon dioxide (100 mL/min) was carried out to commence the process of adsorption maintained for 60 minutes. To facilitate desorption, the sample was thereafter exposed to thermal treatment at a temperature of 100 °C under a continuous flow of nitrogen gas (100 mL/min) for 150 minutes. This process aimed at eliminating the adsorbed carbon dioxide from the sample. These processes of adsorption and desorption were carried out for five cycles.

4. Conclusions

Enhanced CO_2 adsorption and selectivity were observed in composites made by encapsulating two amino acid-based ionic liquids (AAILs) within the highly porous metal-organic framework, MOF-177. The composite material with a loading of 20 wt.% [Emim][Gly] demonstrated the highest recorded CO_2 uptake of 0.45 $mmol \cdot g^{-1}$ solid at a pressure of 0.2 bar and 303 K. The composite material with 20 wt.% [Emim][Ala] exhibited a CO_2 uptake of 0.42 $mmol \cdot g^{-1}$ solid, of 3 and 2.8 times higher than the CO_2 uptake of pure MOF-177. The introduction of AAILs resulted in an enhancement of the CO_2/N_2 selectivity, with values increasing from 5 (for the pure MOF-177) to 13 for [Emim][Gly] and 11 for [Emim][Ala] at a pressure of 0.2 bar and a temperature of 313 K. The interaction between carbon dioxide and the amino ($-NH_2$) functional group, facilitated by the anion of the amino acid ionic liquids (AAILs) resulted in increased adsorption enthalpy (Q_{st}) values. Q_{st} values for the pure MOF-177 remained relatively stable at 13 $kJ \cdot mol^{-1}$, in contrast, a significant rise in Q_{st} was observed for the composites, particularly at low levels of CO_2 uptake. When compared to other [Emim][Gly] composites, 20-[Emim][Gly]@MOF-177 showed the highest values for Qst, reaching a maximum of -28 $kJ \cdot mol^{-1}$ at 0.2 $mmol \cdot g^{-1}$ CO_2 uptake. The present investigation also revealed that the ideal loading of AAIL was 20 wt.%, whereas any subsequent increase in loading to 30 wt.% was inadvisable. At a loading of 30 wt.% the decline in CO_2 absorption could potentially be attributed to a reduction in the availability of active sites on the sorbent. This reduction may be caused by the blockage or the collapse of the MOF-177 structure, as evidenced by a decrease in both surface area and pore volume. The X-ray diffraction (XRD) examination revealed that the introduction of higher amounts of AAIL led to a loss in the structural integrity of the original support material.

This study provides insights into the structural integrity of AAILs@MOF-177 composites, as well as their performance in terms of CO_2 capture and CO_2/N_2 selectivity, and adsorption enthalpies in post-combustion CO_2 capture processes.

Author Contributions: Firuz A. Philip: Conceptualization, Methodology, Material synthesis, Characterization, Experimental analysis, Validation, Data analysis, Writing-Original draft preparation, **Amr Henni**: Conceptualization, Resources, Funding acquisition, Writing-Review& Editing, Project administration, Supervision, A. H. (Amr Henni)

Funding: This research was funded by a grant provided to the second author by The Natural Sciences and Engineering Research Council of Canada (**NSERC**)- Discovery Grant (RGPIN-2018-06805)

Institutional Review Board Statement: Not applicable

Informed Consent Statement: Not applicable

Data Availability Statement: The data presented in this study are available on request from the corresponding author.

Acknowledgments: The authors are grateful to Dr. Golam Kibria's lab (University of Calgary) for providing support for some sample characterizations.

Conflicts of Interest: The authors declare no conflict of interest.

Sample Availability: Samples of the compounds are not available from the authors.

References

1. Sumida, K.; Rogow, D.L.; Mason, J.A.; McDonald, T.M.; Bloch, E.D.; Herm, Z.R.; Bae, T.H.; Long, J.R. Carbon Dioxide Capture in Metal-Organic Frameworks. *Chem. Rev.* **2012**, *112*, 724–781, doi:10.1021/cr2003272.
2. Lin, Y.; Kong, C.; Zhang, Q.; Chen, L. Metal-Organic Frameworks for Carbon Dioxide Capture and Methane Storage. *Adv. Energy Mater.* **2017**, *7*, 1601296, doi:10.1002/aenm.201601296.
3. Hu, Z.; Wang, Y.; Shah, B.B.; Zhao, D. CO_2 Capture in Metal-Organic Framework Adsorbents: An Engineering Perspective. *Adv. Sustain. Syst.* **2018**, *3*, 1800080, doi:10.1002/adsu.201800080.
4. Aghaie, M.; Rezaei, N.; Zendehboudi, S. A Systematic Review on CO_2 Capture with Ionic Liquids: Current Status and Future Prospects. *Renew. Sustain. Energy Rev.* 2018, *96*, 502–525.
5. Yu, J.; Xie, L.H.; Li, J.R.; Ma, Y.; Seminario, J.M.; Balbuena, P.B. CO_2 Capture and Separations Using MOFs: Computational and Experimental Studies. *Chem. Rev.* 2017, *117*, 9674–9754.
6. Belmabkhout, Y.; Guillerm, V.; Eddaoudi, M. Low Concentration CO_2 Capture Using Physical Adsorbents: Are Metal-Organic Frameworks Becoming the New Benchmark Materials? *Chem. Eng. J.* 2016, *296*, 386–397.
7. Yin, Z.; Wan, S.; Yang, J.; Kurmoo, M.; Zeng, M.H. Recent Advances in Post-Synthetic Modification of Metal–Organic Frameworks: New Types and Tandem Reactions. *Coord. Chem. Rev.* 2019, *378*, 500–512.
8. Jasuja, H.; Walton, K.S. Experimental Study of CO_2, CH_4, and Water Vapor Adsorption on a Dimethyl-Functionalized UiO-66 Framework. *J. Phys. Chem. C* **2013**, *117*, 7062–7068, doi:10.1021/jp311857e.
9. Cmarik, G.E.; Kim, M.; Cohen, S.M.; Walton, K.S. Tuning the Adsorption Properties of Uio-66 via Ligand Functionalization. *Langmuir* **2012**, *28*, 15606–15613, doi:10.1021/la3035352.
10. Shearer, G.C.; Vitillo, J.G.; Bordiga, S.; Svelle, S.; Olsbye, U.; Lillerud, K.P. Functionalizing the Defects: Postsynthetic Ligand Exchange in the Metal Organic Framework UiO-66. *Chem. Mater.* **2016**, *28*, 7190–7193, doi:10.1021/acs.chemmater.6b02749.
11. Mutyala, S.; Yakout, S.M.; Ibrahim, S.S.; Jonnalagadda, M.; Mitta, H. Enhancement of CO_2 Capture and Separation of CO2/N2 Using Post-Synthetic Modified MIL-100(Fe). *New J. Chem.* **2019**, *43*, 9725–9731, doi:10.1039/c9nj02258a.
12. Su, X.; Bromberg, L.; Martis, V.; Simeon, F.; Huq, A.; Hatton, T.A. Postsynthetic Functionalization of Mg-MOF-74 with Tetraethylenepentamine: Structural Characterization and Enhanced CO_2 Adsorption. *ACS Appl. Mater. Interfaces* **2017**, *9*, 11299–11306, doi:10.1021/acsami.7b02471.
13. Lin, Y.; Yan, Q.; Kong, C.; Chen, L. Polyethyleneimine Incorporated Metal-Organic Frameworks Adsorbent for Highly Selective CO_2 Capture. *Sci. Rep.* **2013**, *3*, doi:10.1038/srep01859.
14. Choi, S.; Watanabe, T.; Bae, T.H.; Sholl, D.S.; Jones, C.W. Modification of the Mg/DOBDC MOF with Amines to Enhance CO 2 Adsorption from Ultradilute Gases. *J. Phys. Chem. Lett.* **2012**, *3*, 1136–1141, doi:10.1021/jz300328j.
15. Fujie, K.; Kitagawa, H. Ionic Liquid Transported into Metal-Organic Frameworks. *Coord. Chem. Rev.* 2016, *307*, 382–390.

16. Adil, K.; Bhatt, P.M.; Belmabkhout, Y.; Abtab, S.M.T.; Jiang, H.; Assen, A.H.; Mallick, A.; Cadiau, A.; Aqil, J.; Eddaoudi, M. Valuing Metal–Organic Frameworks for Postcombustion Carbon Capture: A Benchmark Study for Evaluating Physical Adsorbents. *Adv. Mater.* **2017**, *29*, doi:10.1002/adma.201702953.
17. Kulak, H.; Polat, H.M.; Kavak, S.; Keskin, S.; Uzun, A. Improving CO_2 Separation Performance of MIL-53(Al) by Incorporating 1-n-Butyl-3-Methylimidazolium Methyl Sulfate. *Energy Technol.* **2019**, doi:10.1002/ente.201900157.
18. Kinik, F.P.; Altintas, C.; Balci, V.; Koyuturk, B.; Uzun, A.; Keskin, S. [BMIM][PF6] Incorporation Doubles CO2 Selectivity of ZIF-8: Elucidation of Interactions and Their Consequences on Performance. *ACS Appl. Mater. Interfaces* **2016**, *8*, 30992–31005, doi:10.1021/acsami.6b11087.
19. Koyuturk, B.; Altintas, C.; Kinik, F.P.; Keskin, S.; Uzun, A. Improving Gas Separation Performance of ZIF-8 by [BMIM][BF4] Incorporation: Interactions and Their Consequences on Performance. *J. Phys. Chem. C* **2017**, *121*, 10370–10381, doi:10.1021/acs.jpcc.7b00848.
20. Bates, E.D.; Mayton, R.D.; Ntai, I.; Davis, J.H. CO_2 Capture by a Task-Specific Ionic Liquid. *J. Am. Chem. Soc.* **2002**, *124*, 926–927, doi:10.1021/ja017593d.
21. Fukumoto, K.; Yoshizawa, M.; Ohno, H. Room Temperature Ionic Liquids from 20 Natural Amino Acids. *J. Am. Chem. Soc.* **2005**, *127*, 2398–2399, doi:10.1021/ja043451i.
22. Sistla, Y.S.; Khanna, A. CO_2 Absorption Studies in Amino Acid-Anion Based Ionic Liquids. *Chem. Eng. J.* **2015**, *273*, 268–276, doi:10.1016/j.cej.2014.09.043.
23. Muhammad, N.; Man, Z.B.; Bustam, M.A.; Mutalib, M.I.A.; Wilfred, C.D.; Rafiq, S. Synthesis and Thermophysical Properties of Low Viscosity Amino Acid-Based Ionic Liquids. *J. Chem. Eng. Data* **2011**, *56*, 3157–3162, doi:10.1021/je2002368.
24. Zhang, J.; Zhang, S.; Dong, K.; Zhang, Y.; Shen, Y.; Lv, X. Supported Absorption of CO_2 by Tetrabutylphosphonium Amino Acid Ionic Liquids. *Chem. - A Eur. J.* **2006**, *12*, 4021–4026, doi:10.1002/chem.200501015.
25. Wang, X.; Akhmedov, N.G.; Duan, Y.; Luebke, D.; Hopkinson, D.; Li, B. Amino Acid-Functionalized Ionic Liquid Solid Sorbents for Post-Combustion Carbon Capture. *ACS Appl. Mater. Interfaces* **2013**, *5*, 8670–8677, doi:10.1021/am402306s.
26. Uehara, Y.; Karami, D.; Mahinpey, N. CO_2 Adsorption Using Amino Acid Ionic Liquid-Impregnated Mesoporous Silica Sorbents with Different Textural Properties. *Microporous Mesoporous Mater.* **2019**, *278*, 378–386, doi:10.1016/j.micromeso.2019.01.011.
27. Uehara, Y.; Karami, D.; Mahinpey, N. Amino Acid Ionic Liquid-Modified Mesoporous Silica Sorbents with Remaining Surfactant for CO_2 Capture. *Adsorption* **2019**, *1*, 703–716, doi:10.1007/s10450-019-00053-1.
28. Philip, F.A.; Henni, A. Enhancement of Post-Combustion CO_2 Capture Capacity by Incorporation of Task-Specific Ionic Liquid into ZIF-8. *Microporous Mesoporous Mater.* **2021**, 111580, doi:10.1016/j.micromeso.2021.111580.
29. Furukawa, H.; Miller, M.A.; Yaghi, O.M. Independent Verification of the Saturation Hydrogen Uptake in MOF-177 and Establishment of a Benchmark for Hydrogen Adsorption in Metal-Organic Frameworks. *J. Mater. Chem.* **2007**, *17*, 3197–3204, doi:10.1039/b703608f.
30. Mohamedali, M.; Henni, A.; Ibrahim, H. Investigation of CO_2 Capture Using Acetate-Based Ionic Liquids Incorporated into Exceptionally Porous Metal–Organic Frameworks. *Adsorption* **2019**, *25*, 675–692, doi:10.1007/s10450-019-00073-x.
31. Saha, D.; Deng, S. Structural Stability of Metal Organic Framework MOF-177. *J. Phys. Chem. Lett.* **2010**, *1*, 73–78, doi:10.1021/jz900028u.
32. Li, Y.; Yang, R.T. Gas Adsorption and Storage in Metal-Organic Framework MOF-177. *Langmuir* **2007**, *23*, 12937–12944, doi:10.1021/la702466d.
33. Santos, K.M.C.; Santos, R.J.O.; De Araújo Alves, M.M.; De Conto, J.F.; Borges, G.R.; Dariva, C.; Egues, S.M.; Santana, C.C.; Franceschi, E. Effect of High Pressure CO_2 Sorption on the Stability of Metalorganic Framework MOF-177 at Different Temperatures. *J. Solid State Chem.* **2019**, *269*, 320–327, doi:10.1016/j.jssc.2018.09.046.
34. Saha, D.; Wei, Z.; Deng, S. Equilibrium, Kinetics and Enthalpy of Hydrogen Adsorption in MOF-177. *Int. J. Hydrogen Energy* **2008**, *33*, 7479–7488, doi:10.1016/j.ijhydene.2008.09.053.
35. Ren, J.; Wu, L.; Li, B.G. Preparation and CO_2 Sorption/Desorption of N -(3-Aminopropyl)Aminoethyl Tributylphosphonium Amino Acid Salt Ionic Liquids Supported into Porous Silica Particles. *Ind. Eng. Chem. Res.* **2012**, *51*, 7901–7909, doi:10.1021/ie2028415.
36. Gurkan, B.E.; De La Fuente, J.C.; Mindrup, E.M.; Ficke, L.E.; Goodrich, B.F.; Price, E.A.; Schneider, W.F.; Brennecke, J.F. Equimolar CO_2 Absorption by Anion-Functionalized Ionic Liquids. *J. Am. Chem. Soc.* **2010**, *132*, 2116–2117, doi:10.1021/ja909305t.
37. Wang, X.; Akhmedov, N.G.; Duan, Y.; Luebke, D.; Li, B. Immobilization of Amino Acid Ionic Liquids into Nanoporous Microspheres as Robust Sorbents for CO_2 Capture. *J. Mater. Chem. A* **2013**, *1*, 2978–2982, doi:10.1039/c3ta00768e.

38. Ferreira, T.J.; Ribeiro, R.P.P.L.; Mota, J.P.B.; Rebelo, L.P.N.; Esperança, J.M.S.S.; Esteves, I.A.A.C. Ionic Liquid-Impregnated Metal-Organic Frameworks for CO_2/CH_4 Separation. *ACS Appl. Nano Mater.* **2019**, *2*, 7933–7950, doi:10.1021/acsanm.9b01936.
39. Sumida, K.; Rogow, D.L.; Mason, J.A.; McDonald, T.M.; Bloch, E.D.; Herm, Z.R.; Bae, T.-H.; Long, J.R. Carbon Dioxide Capture in Metal–Organic Frameworks. *Chem. Rev.* **2012**, *112*, 724–781, doi:10.1021/cr2003272.
40. Mohamedali, M.; Ibrahim, H.; Henni, A. Incorporation of Acetate-Based Ionic Liquids into a Zeolitic Imidazolate Framework (ZIF-8) as Efficient Sorbents for Carbon Dioxide Capture. *Chem. Eng. J.* **2018**, *334*, 817–828, doi:10.1016/J.CEJ.2017.10.104.